

Supplementary Information

A Multifunctional Microporous Metal–Organic Framework: Efficient Adsorption of Iodine and Column-chromatographic Dye Separation

Chan Yao,^a Wei Wang,^a Shu-Ran Zhang,^a Hui-Ying Li,^a Yan-Hong Xu,^{*a,b}

Zhong-Min Su^c and Guang-Bo Che^{*a}

^a Key Laboratory of Preparation and Applications of Environmental Friendly Materials (Jilin Normal University), Ministry of Education, Changchun 130103, Jilin, People's Republic of China

^b Key Laboratory of Functional Materials Physics and Chemistry of the Ministry of Education, Jilin Normal University, Siping 136000, Jilin, People's Republic of China

^c Institute of Functional Material Chemistry, Faculty of Chemistry, Northeast Normal University, Changchun, 130024, Jilin, People's Republic of China

Table S1 Crystal data and structure refinements for **JLNU-4**.

Identification code	JLNU-4
Formula	C ₃₆ H ₅₁ N ₇ O ₁₅ Cd ₂
Formula weight	1046.65
Crystal system	Monoclinic
Space group	<i>P2</i> ₁ / <i>c</i>
<i>a</i> (Å)	14.3590(9)
<i>b</i> (Å)	14.4350(10)
<i>c</i> (Å)	22.6110(14)
α (°)	90
β (°)	98.6970(11)
γ (°)	90
<i>V</i> (Å ³)	4632.7(5)
<i>Z</i>	4
<i>D</i> _{calcd} [g cm ⁻³]	1.001
<i>F</i> (000)	1360
Reflections collected	25012 / 9129
<i>R</i> (int)	0.0463
Goodness-of-fit on <i>F</i> ²	1.097
<i>R</i> ₁ ^a [<i>I</i> > 2σ(<i>I</i>)]	0.0781
<i>wR</i> ₂ ^b	0.2803

$${}^a R_1 = \sum \|F_o\| - |F_c| / \sum |F_o|, \quad {}^b wR_2 = \left| \sum w(|F_o|^2 - |F_c|^2) \right| / \sum |w(F_o^2)|^{1/2}.$$

Table S2 The selected bond lengths for **JLNU-4**.

JLNU-4			
O(1)-Cd(1)	2.301(6)	O(6)-Cd(2)	2.244(7)
O(1)-Cd(2)	2.307(6)	O(7)-Cd(1)	2.276(7)
O(2)-Cd(1)	2.570(7)	O(8)-Cd(2)	2.308(9)
O(3)-Cd(1)	2.415(6)	O(9)-Cd(2)	2.235(12)
O(4)-Cd(1)	2.276(6)	O(10)-Cd(2)	2.235(8)
O(5)-Cd(1)	2.213(6)	O(11)-Cd(2)	2.269(13)

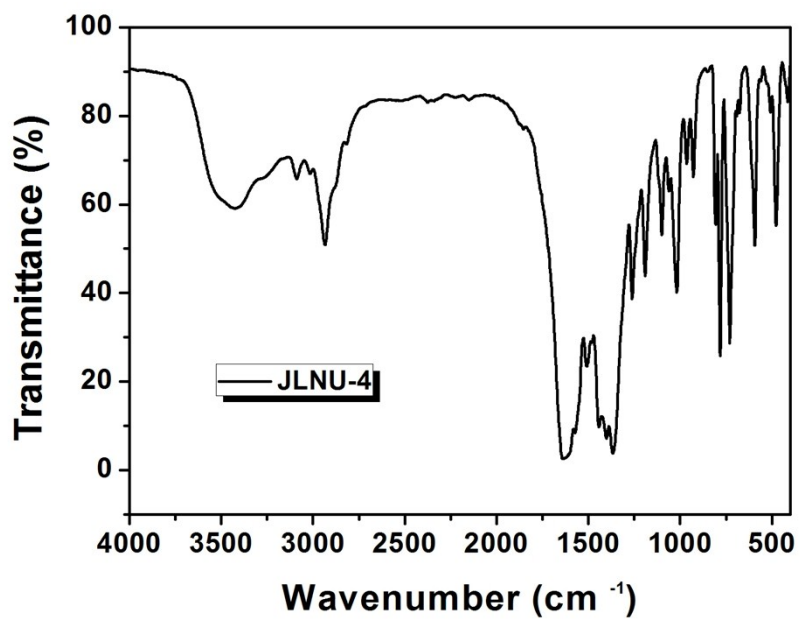


Fig. S1 The IR spectrum of JLNU-4 in KBr pellets from 4000 cm^{-1} to 400 cm^{-1} .

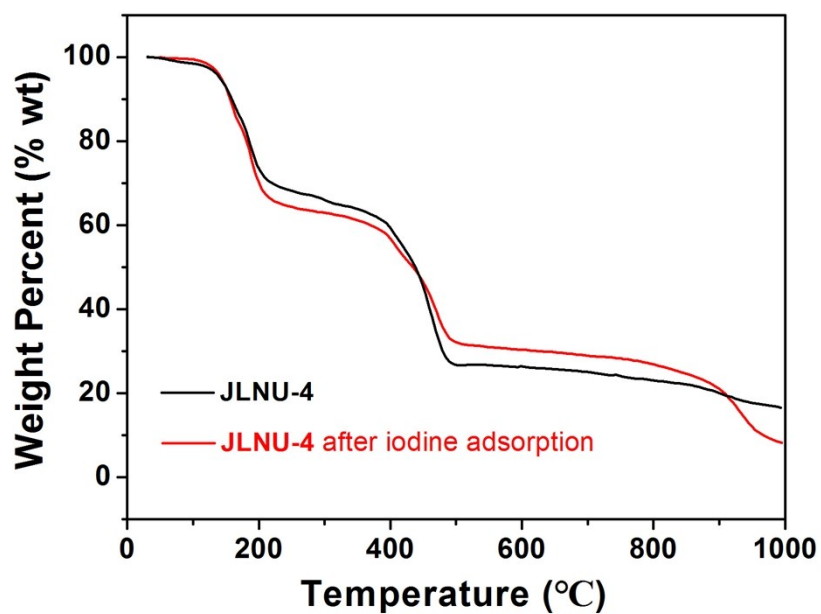


Fig. S2 The TGA curve of (a) JLNU-4 and (b) JLNU-4 after iodine adsorption measured under N_2 atmosphere from 40 to 1000 $^{\circ}\text{C}$ at the heating rate of 10 $^{\circ}\text{C}\cdot\text{min}^{-1}$.

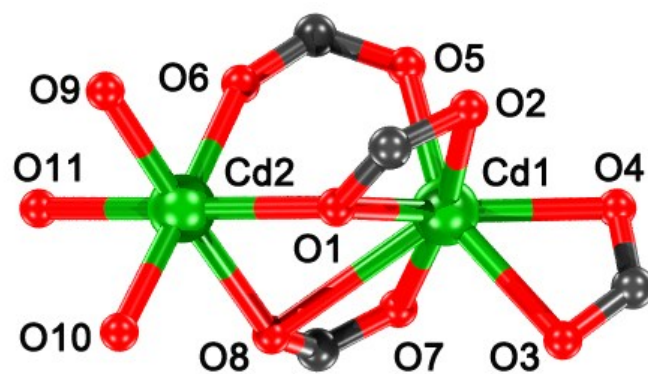


Fig. S3 Ball-and-stick representation of a binuclear $[\text{Cd}_2(\text{CO})_4(\text{H}_2\text{O})_2(\text{DMA})]$ cluster in JLNU-4.

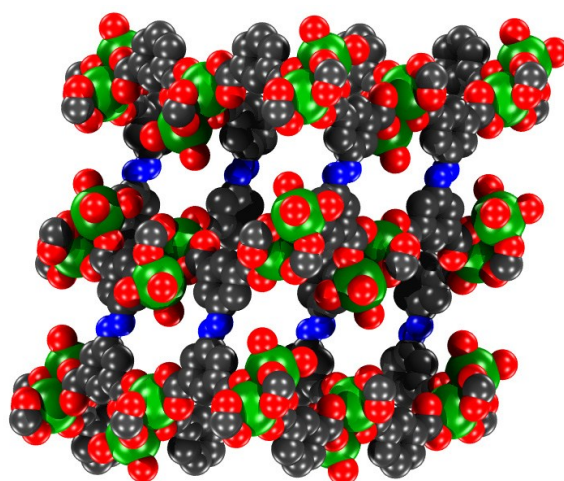


Fig. S4 Space-filling representation of the packing arrangement for the 3D structure in JLNU-4.

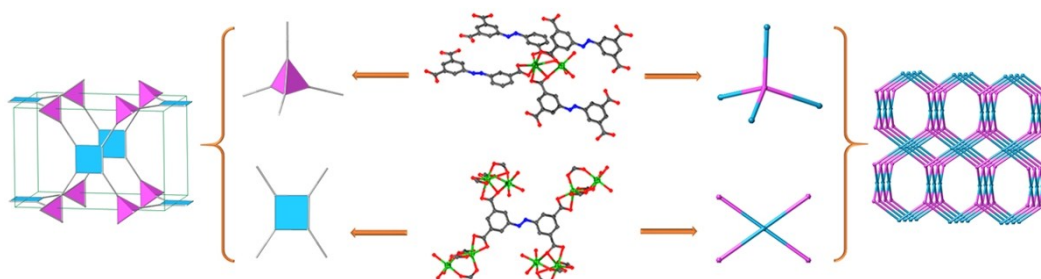


Fig. S5 Polyhedral and ball-and-stick view of the (4,4)-connected topology network in JLNU-4.

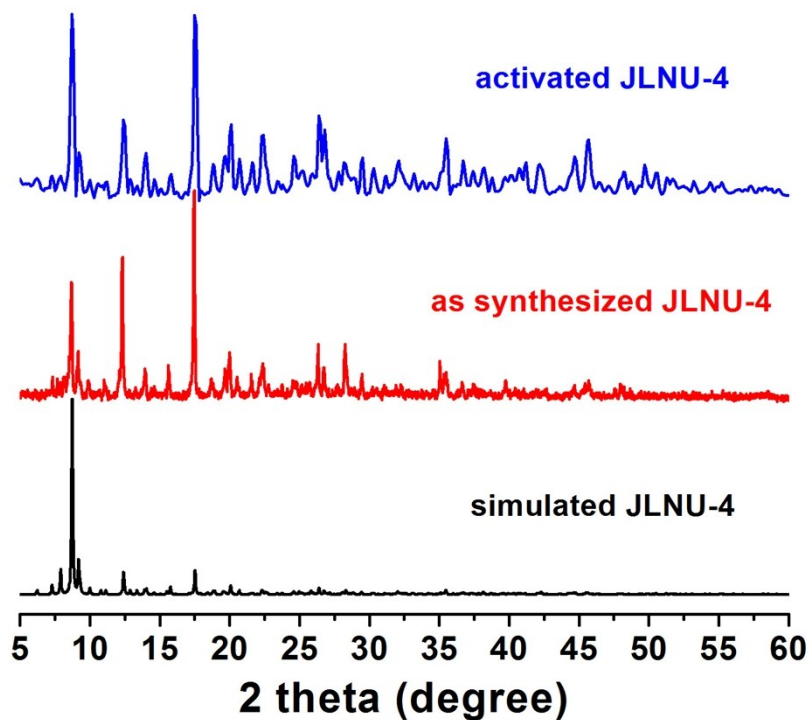


Fig. S6 PXRD patterns of simulated JLNU-4 (black), as-synthesized JLNU-4 (red) and activated JLNU-4 (blue).

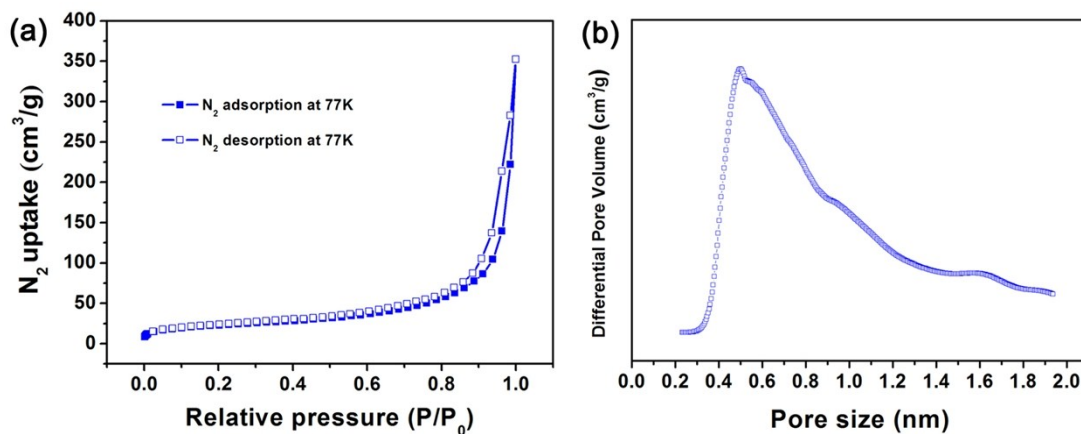


Fig. S7 (a) The N_2 gas-sorption isotherms of JLNU-4 measured at 77 K, 1 atm. (b) The pore size distribution of JLNU-4 calculated using density functional theory (DFT) method.

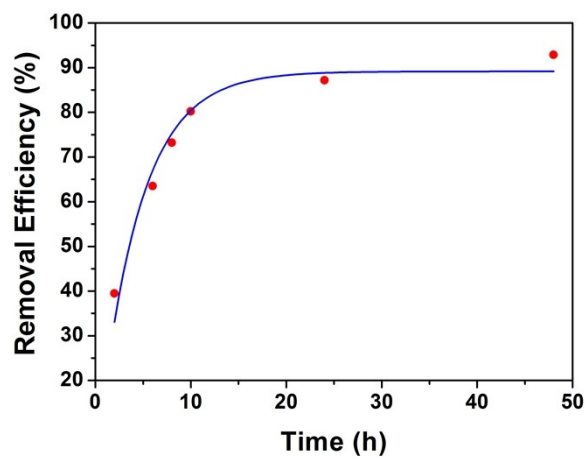


Fig. S8 The iodine adsorption kinetic was analyzed by the pseudo-first-order kinetic model. The initial concentration of iodine solution is $4 \text{ mg}\cdot\text{mL}^{-1}$.

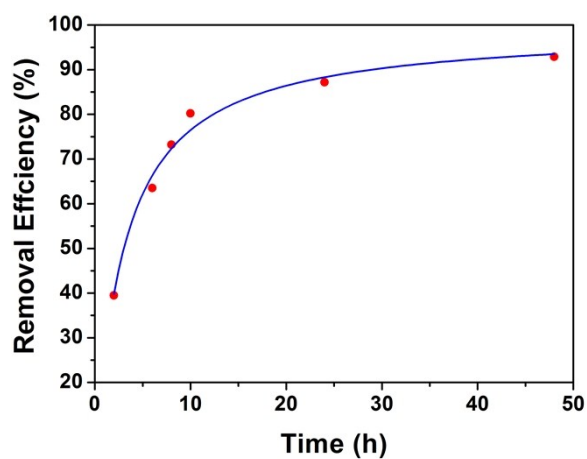


Fig. S9 The iodine adsorption kinetic was analyzed by the pseudo-second-order kinetic model. The initial concentration of iodine solution is $4 \text{ mg}\cdot\text{mL}^{-1}$.

Table S3 Parameters of the iodine adsorption kinetic analyzed by the pseudo-first-order model and pseudo-second-order model for **JLNU-4**.

Pseudo-first-order			Pseudo-second-order		
$k_1 \text{ (h}^{-1}\text{)}$	$Q_e \text{ (%)}$	R^2	$k_2 \text{ (h}^{-1}\text{)}$	$Q_e \text{ (%)}$	R^2
0.2318	89.166	0.95034	0.00337	99.3008	0.9837

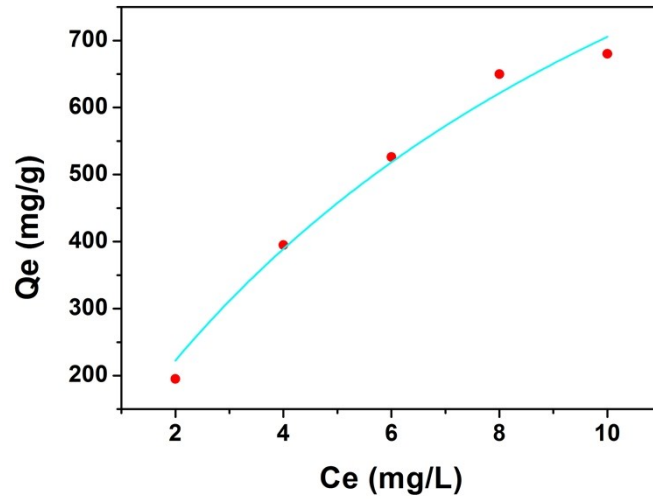


Fig. S10 The Langmuir adsorption isotherm of the iodine adsorption for **JLNU-4**.

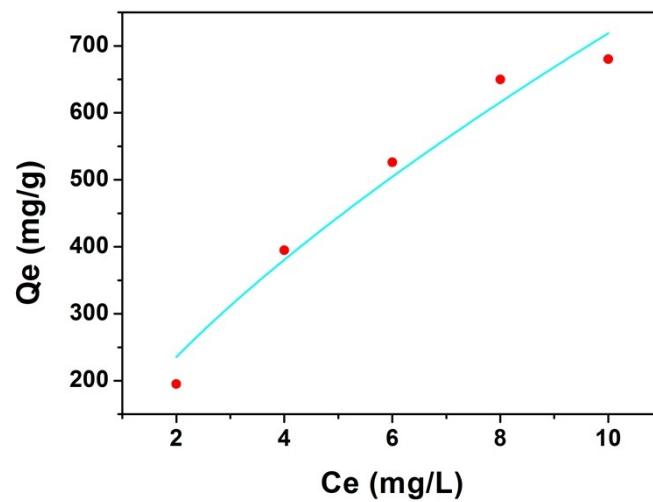


Fig. S11 The Freundlich adsorption isotherm of the iodine adsorption for **JLNU-4**.

Table S4 Parameters of two different simulation models extracted from experimental adsorption isotherms data for **JLNU-4**.

Langmuir adsorption isotherm			Freundlich adsorption isotherm		
Q_m (mg·g ⁻¹)	k_L (mg ⁻¹)	R^2	k_F (mg ⁻¹)	n	R^2
1540.464	0.08449	0.98043	145.484	1.44124	0.95821

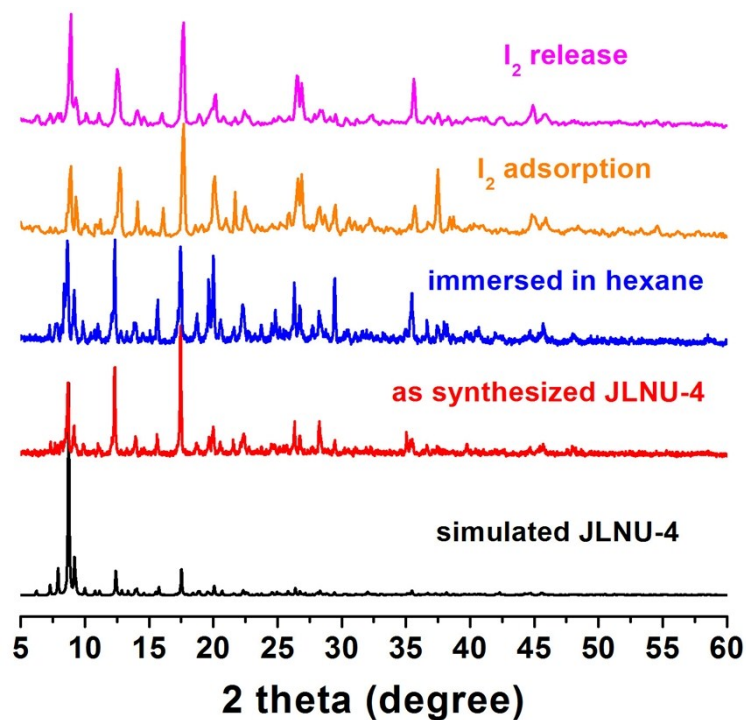


Fig. S12 PXRD patterns of simulated **JLNU-4** (black), as-synthesized **JLNU-4** (red), immersed in hexane solution (blue), as-synthesized **JLNU-4** after iodine adsorption and release.

Table S5 The gravimetric measurement of **JLNU-4** during the iodine adsorption in vapor phase at a time interval.^a

Time interval	Weight (g)
0	5.8156
2	5.8266
4	5.8301
6	5.8330
8	5.8339
10	5.8347
12	5.8347
14	5.8348

^aThe weight measured at a time interval was the total mass of **JLNU-4** and the vessel, in which the initial weight of **JLNU-4** was 30 mg.

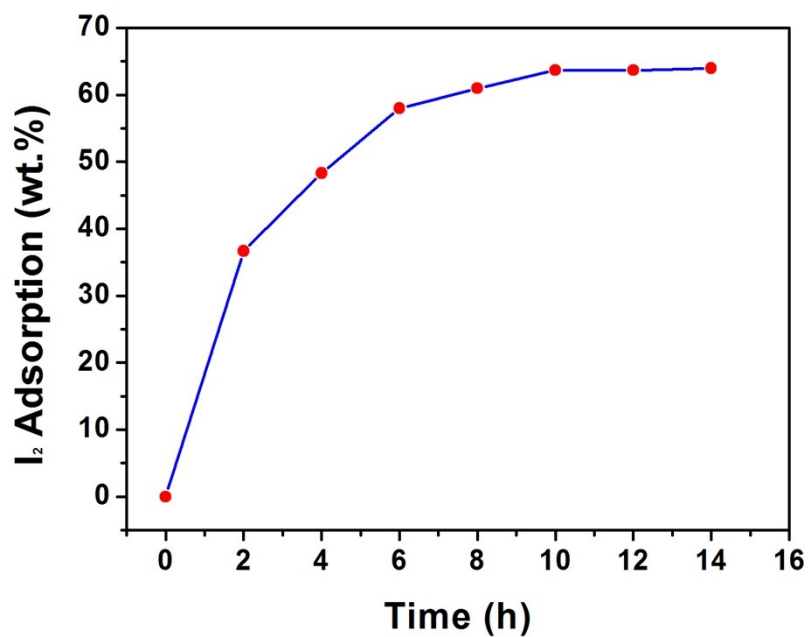


Fig. S13 Gravimetric uptake of iodine for JLNU-4 as a function of time at 350 K.

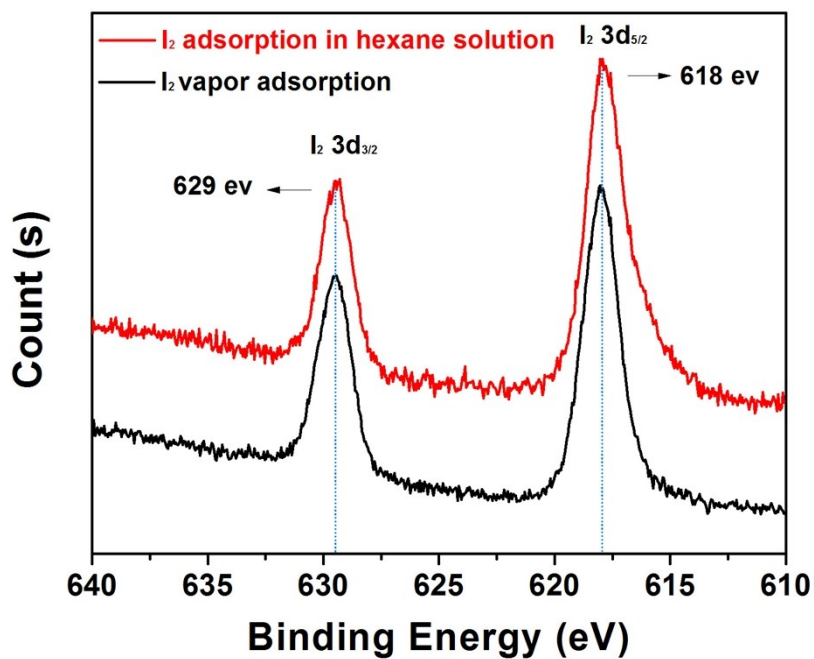


Fig. S14 XPS spectrum of JLNU-4 after iodine adsorption in hexane solution and iodine vapor adsorption, respectively.

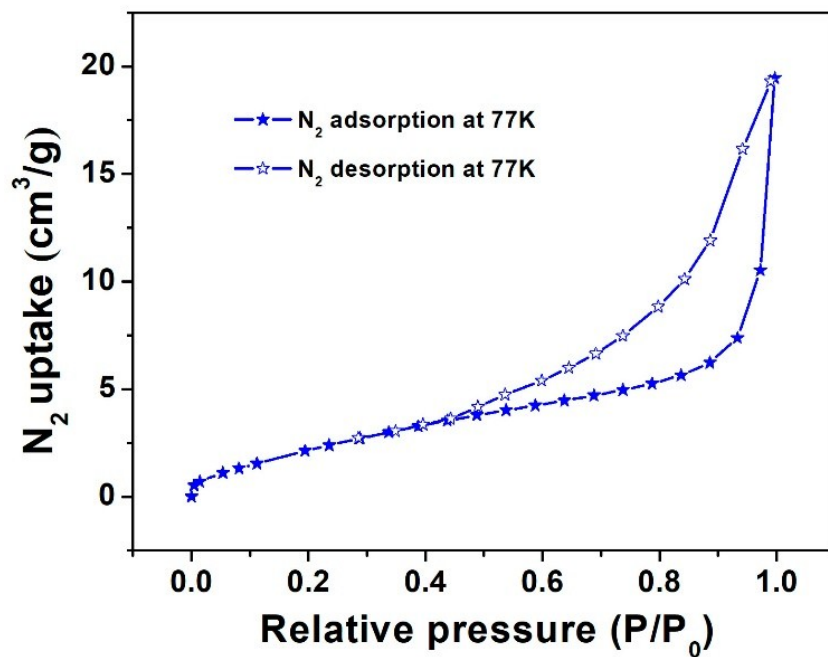


Fig. S15 The N₂ gas-sorption isotherms of MB loaded JLNU-4 measured at 77 K, 1 atm.

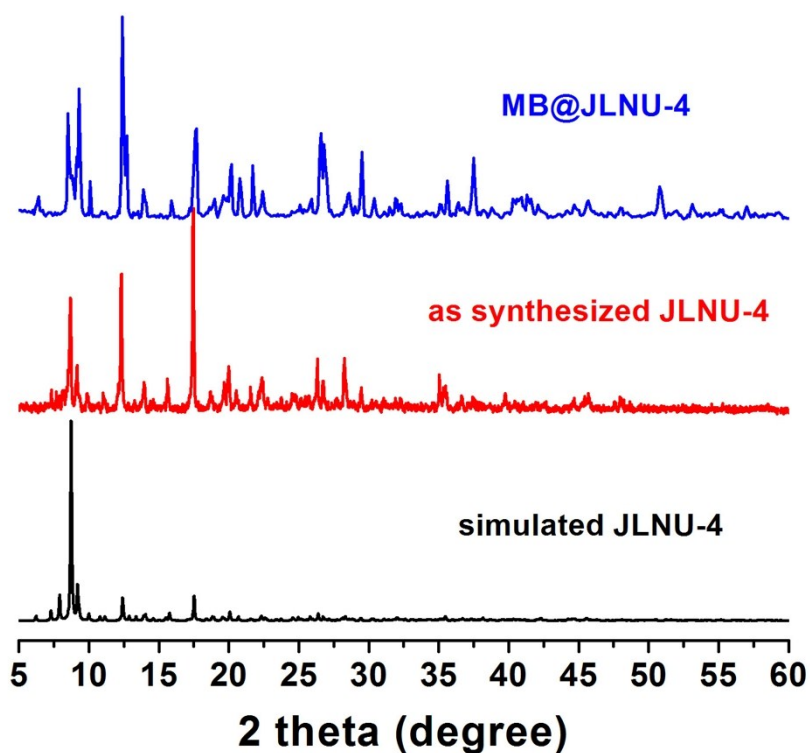


Fig. S16 XRPD patterns of simulated JLNU-4 (black), as-synthesized JLNU-4 (red) and after the absorption of MB (blue), respectively.

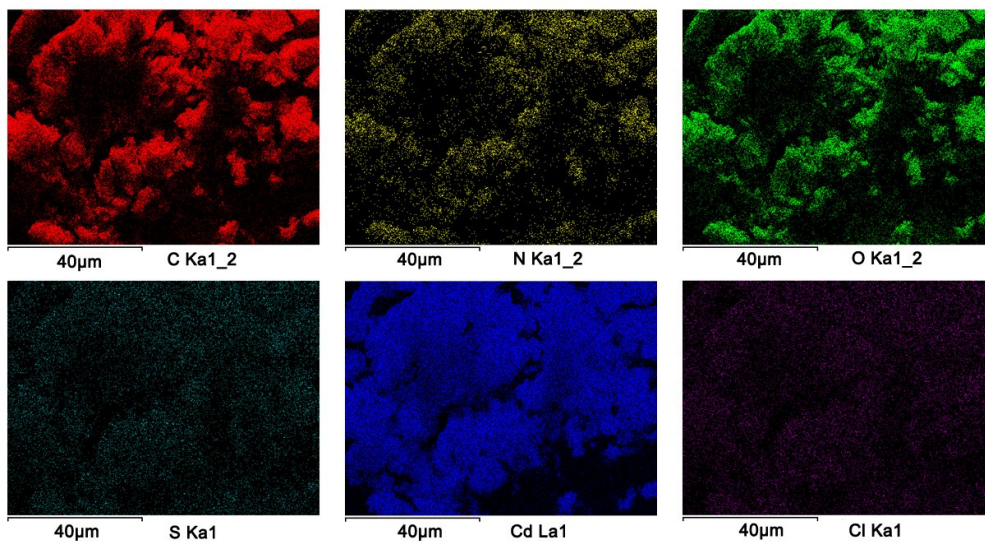


Fig. S17 EDS images of MB loaded JLNU-4.

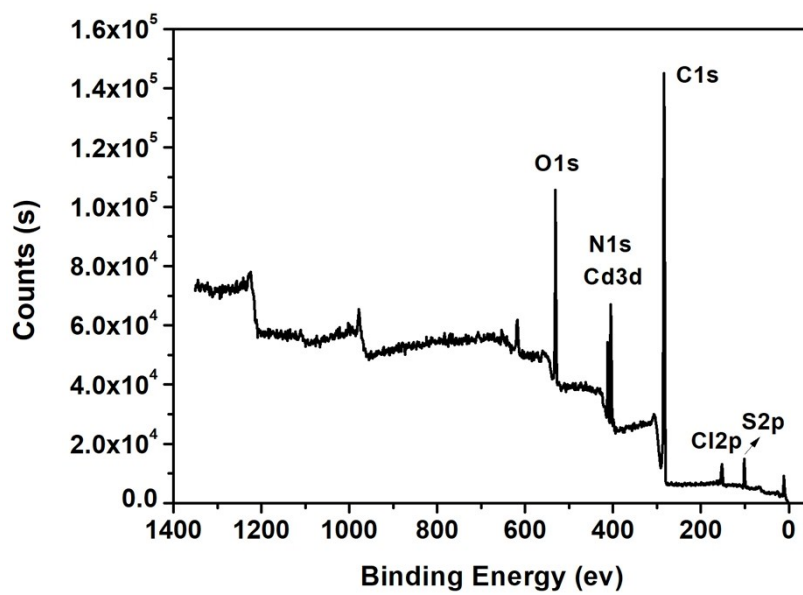


Fig. S18 XPS spectrum of contained elements for MB loaded JLNU-4.

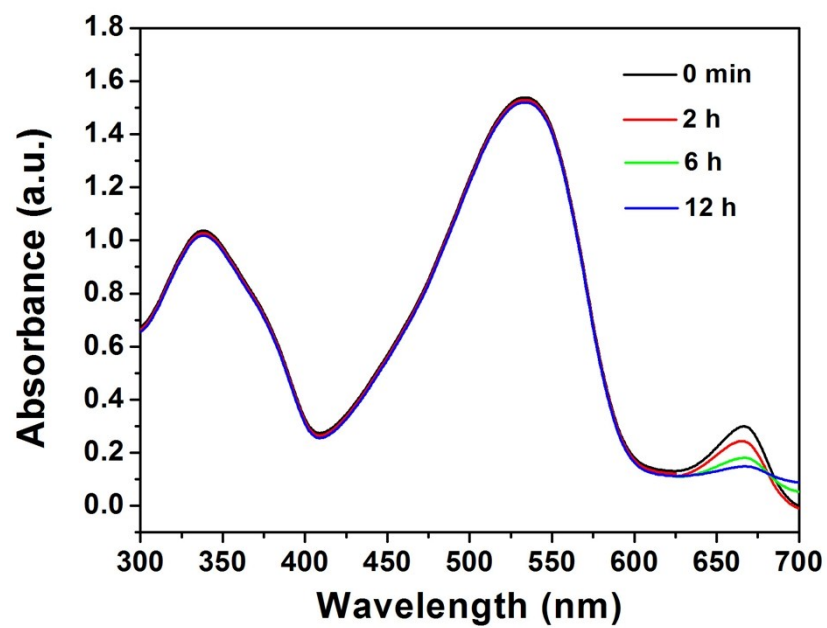


Fig. S19 UV/vis spectra of the effluent during the dye mixture of MB and CR passing through the MOF-filled chromatographic column.